Chiral anomaly and the pion transition form factor: Beyond the cutoff

Hao Dang [1,*] Zanbin Xing,[1,†] M. Atif Sultan,[1,2,‡] Khépani Raya[3,§] and Lei Chang[1,‖]

[1]*School of Physics, Nankai University, Tianjin 300071, China*
[2]*Centre For High Energy Physics, University of the Punjab, Lahore 54590, Pakistan*
[3]*Department of Integrated Sciences and Center for Advanced Studies in Physics,*
Mathematics and Computation, University of Huelva, E-21071 Huelva, Spain

In the presence of a momentum cutoff, effective theories seem unable to faithfully reproduce the so-called chiral anomaly in the Standard Model. A novel prospect to overcome this related issue is discussed herein via the calculation of the $\gamma^* \pi^0 \gamma$ transition form factor $G^{\gamma^* \pi^0 \gamma}(Q^2)$, whose normalization is intimately connected with the chiral anomaly and dynamical chiral symmetry breaking (DCSB). To compute such transition, we employ a contact interaction model of quantum chromodynamics (QCD) under a modified rainbow ladder truncation, which automatically generates a quark anomalous magnetic moment term, weighted by a strength parameter ξ. This term, whose origin is also connected with DCSB, is interpreted as an additional interaction that mimics the complex dynamics beyond the cutoff. By fixing ξ to produce the value of $G^{\gamma^* \pi^0 \gamma}(0)$ dictated by the chiral anomaly, the computed transition form factor, as well as the interaction radius and neutral pion decay width, turn out to be comparable with QCD-based studies and experimental data.

I. INTRODUCTION

Conserved currents in classical theory may be violated by quantum corrections, an outcome referred to as anomaly. One of the most notable anomalies in the Standard Model is the chiral anomaly discovered in 1969 by Adler [1] and Bell and Jackiw [2], which is responsible for the neutral pion decay, thereby having a significant impact in the $\gamma^* \pi^0 \gamma$ transition form factor (TFF). In addressing this transition process, there is a long-standing problem in effective theories such as Nambu–Jona-Lasinio-like theories; namely, the anomalous neutral pion decay is smaller than the experimental value in the presence of a finite cutoff [3,4], and the difference between theory and experiment relies on the regularization scheme. This problem is discussed extensively but there is not a completely satisfactory solution, see Refs. [3–7]. For instance, if the cutoff is removed, the chiral anomaly is faithfully reproduced [8]. Nonetheless, one could argue that the cutoff itself is part of the effective theory and thus should not be changed nor removed in the calculation of observables. On the other hand, the role of the cutoff within a path integral derivation of the chiral anomaly is clarified in Ref. [4], highlighting cutoff-dependent higher-order contributions that are crucial for the chiral anomaly. In principle, it is impossible to explicitly calculate such contributions at all orders without making assumptions. However, as meticulously illustrated in Ref. [9], once the cutoff is introduced in the effective theory, additional local interaction terms should be added to mimic the complex interaction triggered by higher-order contributions that appear at shorter distances (or at higher energies) compared to the cutoff. These additional terms depend on the latter and must vanish upon its removal. This conception, however, has not been implemented so far in any effective theory study involving the chiral anomaly. In this work, we shall adopt these ideas in the calculation of the neutral pion decay and the corresponding $\gamma^* \pi^0 \gamma$ TFF, by using an effective model within the framework of Dyson-Schwinger equations (DSEs), i.e., the contact interaction (CI) model [10,11].

The DSE formalism has proven to be a powerful tool in studying the nonperturbative nature of quantum chromodynamics (QCD) in the continuum [12,13], representing an ideal platform to study the static and structural properties of hadrons [14–18]. Within this framework, the mass spectrum and structural properties of hadrons are governed by the relationship between the quark DSE and the

---

*haodang@mail.nankai.edu.cn
†xingzb@mail.nankai.edu.cn
‡atifsultan.chep@pu.edu.pk
§khepani.raya@dci.uhu.es
‖leichang@nankai.edu.cn

bound-state Bethe-Salpeter (BS) and Faddeev equations [19,20]. In fact, bound-state equations would be related to Green's functions of the theory, in such a way that the resulting infinite system of integral equations must be truncated in a systematic way [21,22]. A popular approach is the so-called symmetry-preserving vector-vector contact interaction, originally introduced to study the properties of the pion [8,10], in a relatively simple framework capable of preserving key features of QCD such as confinement and chiral symmetry breaking. To date, the CI model has been employed to address numerous hadronic properties, including meson and baryon mass spectrum, various decay processes, form factors, and parton distributions (see, e.g., Refs. [8,10,23–36]); the emanating predictions, especially those concerning static properties, have provided valuable benchmarks for both more sophisticated treatments of QCD and experiment.

To properly address meson properties, a consistent truncation of the DSE and BS equation (BSE) is crucial to preserve the symmetries of QCD. The traditional rainbow ladder (RL) truncation is the common choice [37–40], among others, because it properly captures the Goldstone-boson nature of the pion [41,42]. However, embedded within the CI, the RL truncation fails at reproducing the chiral anomaly due to the presence of cutoffs; only when those are removed it is possible to recover the anomaly [8]. A modified RL (MRL) truncation, recently proposed in Refs. [43,44], would represent a feasible alternative. This truncation consistently generates the quark anomalous magnetic moment (AMM) term in the quark-photon vertex (QPV), while maintaining the relevant symmetries of QCD and leaving the pion static properties untouched. Following the spirit of Refs. [4,9], the AMM term can be interpreted as an additional interaction, between quark and photon, which mimics the dynamics beyond the cutoff. As required by this interpretation, we will also see in the following that the AMM term vanishes if one removes the CI-induced momentum cutoff under a proper regularization procedure.

The manuscript is organized as follows: In Sec. II, we briefly introduce the CI under the MRL truncation and expose how the structure of the QPV develops an AMM term. In Sec. III, we discuss the $\gamma^*\pi^0\gamma$ TFF in detail: in particular, its connection with the AMM term in detail, its connection with the chiral anomaly, and associated physical quantities. Conclusions and final remarks are presented in Sec. IV.

II. CONTACT INTERACTION

A natural starting point for the calculation of the $\gamma^*\pi^0\gamma$ transition form factor is the quark DSE. This can be expressed mathematically as follows[1]:

---

[1] We employ a Euclidean metric with $\{\gamma_\mu, \gamma_\nu\} = 2\delta_{\mu\nu}$, $\gamma_\mu^\dagger = \gamma_\mu$, $\gamma_5 = \gamma_4\gamma_1\gamma_2\gamma_3$, and $a \cdot b = \sum_i^4 a_i b_i$. The isospin symmetry is considered throughout this work.

$$S^{-1}(p) = S_0^{-1}(p) + \frac{4}{3}g^2 \int_q D_{\mu\nu}(p-q)\gamma_\mu S(q)\Gamma_\nu^G(q,p),$$
$$(1)$$

where $\int_q \doteq \int \frac{d^4q}{(2\pi)^4}$ denotes a Poincaré invariant integration. The dressed quark propagator is fully characterized by two Dirac structures via

$$S^{-1}(p) = Z^{-1}(p^2)(i\gamma \cdot p + M(p^2)), \qquad (2)$$

such that it maintains an analogy with its tree-level counterpart, $S_0^{-1}(p) = i\gamma \cdot p + m$; here m is the bare quark mass and $M(p^2)$ denotes the so-called mass function. The rest of the ingredients of Eq. (1), also known as the gap equation, are defined as usual: Γ_ν^G and $g^2 D_{\mu\nu}$ represent, respectively, the fully dressed quark-gluon vertex (QGV) and gluon propagator (g is the Lagrangian coupling constant), each of which satisfy their own DSE. This interconnection yields an infinite number of coupled nonlinear integral equations, which must be systematically truncated to study a physical system [45]. Typically, one assumes an appropriate form for the QGV that enable us to arrive at a tractable problem [46,47]. In practice, this also requires replacing the gluon propagator by an effective one $g^2 D_{\mu\nu}(p-q) \to D_{\mu\nu}^{\text{eff}}(p-q)$.

In the CI model, the fully dressed QGV is demoted to its tree-level form, $\Gamma_\nu^G \to \gamma_\nu$, corresponding to the *rainbow* approximation of the gap equation. The corresponding effective gluon propagator is defined as [10]

$$g^2 D_{\mu\nu}^{\text{eff}}(p-q) \to \frac{1}{m_G^2}\delta_{\mu\nu}, \qquad (3)$$

where m_G is a gluon mass scale. Thus, the quark gap equation is expressed as

$$S^{-1}(p) = S_0^{-1}(p) + \frac{4}{3m_G^2} \int_q \gamma_\mu S(q)\gamma_\mu. \qquad (4)$$

This integral possesses quadratic divergence that must be regularized in a Poincaré invariant manner. The solution of Eq. (4) then yields a rather simple form for the quark propagator,

$$S^{-1}(p) = i\gamma \cdot p + M, \qquad (5)$$

where the mass function M in Eq. (2) becomes independent of the quark momentum p. Plugging Eq. (5) into Eq. (4), one obtains the following nonlinear integral equation for M:

$$M = m + \frac{16}{3m_G^2} \int_q \frac{M}{q^2 + M^2}. \qquad (6)$$

Herein we adopt the symmetry-preserving regularization schemes described in Ref. [48], which is based on Schwinger's proper time method,

$$I_{-2\alpha}(\mathcal{M}^2) = \int_q \frac{1}{(q^2 + \mathcal{M}^2)^{\alpha+2}}$$

$$= \int_0^\infty d\tau \frac{\tau^{\alpha-1}}{\Gamma(\alpha+2)} \frac{e^{-\tau\mathcal{M}^2}}{16\pi^2}$$

$$\rightarrow \int_{\tau_{uv}^2}^{\tau_{ir}^2} d\tau \frac{\tau^{\alpha-1}}{\Gamma(\alpha+2)} \frac{e^{-\tau\mathcal{M}^2}}{16\pi^2}$$

$$I_{-2\alpha}^R(\mathcal{M}^2) = \frac{1}{16\pi^2} \frac{\Gamma[\alpha, \tau_{uv}^2\mathcal{M}^2] - \Gamma[\alpha, \tau_{ir}^2\mathcal{M}^2]}{\mathcal{M}^{2\alpha}\Gamma(\alpha+2)}, \quad (7)$$

where $\tau_{uv} = 1/\Lambda_{uv}$ and $\tau_{ir} = 1/\Lambda_{ir}$ are ultraviolet (UV) and infrared (IR) regulators, respectively; $\Lambda_{ir} \simeq \Lambda_{\text{QCD}}$ prevents the quark propagator from developing a pole at $q^2 = -M^2$, avoiding quark production thresholds and thus producing a picture compatible with confinement, whereas Λ_{uv} plays a dynamical role setting the scale of all dimensioned quantities. $\Gamma(n, z)$ is the incomplete gamma function. The label R stands for regularized integrals and will be suppressed in the rest of the paper for simplicity. Thus, in terms of the so-called irreducible loop integrals [48], Eq. (6) becomes

$$M = m + \frac{16M}{3m_G^2} I_2(M^2), \quad (8)$$

such that M is obtained by solving Eq. (8).

Mesons are described by the bound-state BSE, whose interaction kernel must be written in a self-consistent manner with the gap equation [21,22]. In the MRL truncation, the meson BSE reads

$$\Gamma_H(P) = -\frac{4}{3m_G^2} \int_q \gamma_\alpha S(q)\Gamma_H(P)S(q-P)\gamma_\alpha$$

$$+ \frac{4\xi}{3m_G^2} \int_q \tilde{\Gamma}_j S(q)\Gamma_H(P)S(q-P)\tilde{\Gamma}_j, \quad (9)$$

where $\Gamma_H(P)$ is the H-meson BS amplitude (BSA), with P being the total momentum of the bound state. Note the first line in Eq. (9), in conjunction with Eq. (4), defines the RL truncation. Conversely, the second line in Eq. (9) contains the nonladder (NL) pieces, $\tilde{\Gamma}_j = \{I_4, \gamma_5, \frac{i}{\sqrt{6}}\sigma_{\alpha\beta}\}$. As discussed in Ref. [43], with these new structures, the relevant symmetries continue to be satisfied and the vector channels are favorably modified; in particular, as it will become evident, the AMM term in the QPV stems from this contribution. Finally, ξ is a strength parameter controlling the relative weight between the RL and NL contributions, such that $\xi = 0$ recovers the traditional RL truncation.

The general form the pion BSA adopts within the CI-MRL truncation is

$$\Gamma_\pi(P) = i\gamma_5 E_\pi(P) + \frac{\gamma_5\gamma \cdot P}{M} F_\pi(P), \quad (10)$$

where E_π, F_π are scalar functions independent of the relative momentum between the valence quark and antiquark. As with the quark propagator, the simple structure of the BSA is a consequence of the CI and the corresponding symmetry-preserving regularization. The process for solving the pion BSE is described in Appendix A.

In order to compute physical observables, the obtained BSA must be canonically normalized. For the pseudoscalar case, the normalization condition reads

$$P_\mu = N_c tr \int_q \Gamma_\pi(-P)S(q)\Gamma_\pi(P)\frac{\partial}{\partial P_\mu}S(q-P). \quad (11)$$

The pion leptonic decay constant may be computed straightforwardly: this is expressible in the following way:

$$f_\pi P_\mu = N_c tr \int_q \gamma_5\gamma_\mu S(q)\Gamma_\pi(P)S(q-P). \quad (12)$$

Notably, our symmetry-preserving scheme ensures the Goldberger-Treiman relations are reproduced [10]. In particular, in the chiral limit ($P^2 = 0 = m$), we have

$$f_\pi E_\pi = M. \quad (13)$$

The computed masses, decay constants, and the normalized BS amplitudes of the π meson in the CI-MRL truncation, as well as the mass function of the dressed quark, are reported in Table I. It is important to highlight that these quantities are independent of the value of ξ since the NL term in MRL does not contribute to the pseudoscalar meson BSE, which is made clear by performing a Fierz transformation on the NL kernel [43] (see also Appendix A). Therefore, the static properties of the pion remains the same as those computed within the CI-RL case. This is by no means the case of the TFF, since it turns out that the NL pieces of the BS kernel influence the vector channels, so that the structure of the QPV changes favorably [43]. This is discussed below.

TABLE I. Computed pion static properties. The model parameters: $m_G = 0.132$ GeV, $\tau_{uv} = 1/0.905$ GeV^{-1}, and $\tau_{ir} = 1/0.24$ GeV$^{-1} \simeq 1/\Lambda_{\text{QCD}}$. Mass units in GeV.

m	M	m_π	f_π	E_π	F_π
0	0.358	0	0.100	3.566	0.458
0.007	0.368	0.140	0.101	3.595	0.475

A. Quark-photon vertex

The inhomogeneous BSE for the QPV $\Gamma_\mu(Q)$ in the MRL truncation is written as

$$\Gamma_\mu(Q) = \gamma_\mu - \frac{4}{3m_G^2} \int_q \gamma_\alpha S(q) \Gamma_\mu(Q) S(q-Q) \gamma_\alpha$$
$$+ \frac{4\xi}{3m_G^2} \int_q \tilde{\Gamma}_j S(q) \Gamma_\mu(Q) S(q-Q) \tilde{\Gamma}_j. \quad (14)$$

The simplicity of the CI model enable us to fully characterize the QPV by three tensor structures, namely,

$$\Gamma_\mu(Q) = \gamma_\mu^L f_L(Q^2) + \gamma_\mu^T f_T(Q^2) + \frac{\sigma_{\mu\nu} Q_\nu}{M} f_A(Q^2), \quad (15)$$

where $\gamma_\mu^T = \gamma_\mu - \frac{\slashed{Q} Q_\mu}{Q^2}$, $\gamma_\mu^L = \gamma_\mu - \gamma_\mu^T$. By solving Eq. (14), one obtains the dressing functions $f_L(Q^2)$, $f_T(Q^2)$, and $f_A(Q^2)$,

$$f_L(Q^2) = 1,$$
$$f_T(Q^2) = -\frac{\mathcal{I}}{\mathcal{K}(C_0^2 M^2 \hat{\xi} + 2\bar{C}_0 \mathcal{I}) - \mathcal{I}},$$
$$f_A(Q^2) = \frac{C_0 M^2 \hat{\xi}}{\mathcal{K}(C_0^2 M^2 \hat{\xi} + 2\bar{C}_0 \mathcal{I}) - \mathcal{I}}; \quad (16)$$

the integrals $C_\alpha, \bar{C}_\alpha$ are defined as follows:

$$C_\alpha(Q^2) = \int_0^1 I_\alpha(\omega(M^2, u, Q^2)) du,$$
$$\bar{C}_\alpha(Q^2) = \int_0^1 u(u-1) I_\alpha(\omega(M^2, u, Q^2)) du, \quad (17)$$

with $\omega = M^2 + u(1-u)Q^2$, $\mathcal{I} = \hat{\xi}(2C_0 M^2 + C_2) - 1$, $\hat{\xi} = \frac{32\xi}{9m_G^2}$, and $\mathcal{K} = \frac{8Q^2}{3m_G^2}$.

Let us now analyze the QPV dressing functions from Eq. (16). First, the longitudinal piece $f_L(Q^2)$ ensures the vertex satisfies the symmetry requirement of the Ward-Green-Takahashi identity [49]. Second, since the tensor structures to which $f_{T/A}$ are attached (namely, γ_μ^T and $\sigma_{\mu\nu} Q_\nu$) also define the BSA of the vector meson, both exhibit the corresponding vector meson pole in the timelike axis. This would also be the case for RL truncation [50], although producing $f_A(Q^2) = 0$ and a shifted vector meson mass due to the influence of the NL pieces in the BS kernel [43]. Notably, the dressing function of the AMM term $f_A(Q^2)$ happens to be proportional to the strength parameter ξ, so that this term vanishes in the $\xi = 0$ limit. It is precisely in this case that one recovers the RL truncation, which indicates that within the CI, the RL is unable to generate an AMM piece naturally; in fact, such term is often added by hand [23,31]. Regarding the asymptotic

falloff of the dressing functions, one observes that $f_T(Q^2 \to \infty) \to 1$ and $f_A(Q^2 \to \infty) \to 0$, so Eqs. (15) and (16) would guarantee that the tree-level result γ_μ is faithfully recovered. Finally, it is worth showing the values of these dressing functions in the $Q^2 = 0$ point,

$$f_L(0) = 1,$$
$$f_T(0) = 1,$$
$$f_A(0) = \frac{\hat{\xi} M^2 I_0(M^2)}{1 - \hat{\xi}(2M^2 I_0(M^2) + I_2(M^2))}. \quad (18)$$

All these features of the $f_{T/A}$ dressing functions become more perceptible in Fig. 1, which depicts their corresponding profiles in a pertinent range of momenta.

As has been stated, the origin of the AMM term is associated with dynamical chiral symmetry breaking (DCSB), which generates quantifiable (albeit with opposite signs) chromo- and electromagnetic moments at infrared momenta [51–53]. This contribution would produce a measurable outcome in transitions involving spin particles, such as the $\gamma^* \rho \to \pi$ case [37], and even critical effects in processes involving excited states of orbital angular momentum, for both mesons and baryons [31]. A prime example of the latter is the electromagnetic transition of the nucleon to its parity partner, whose corresponding Pauli form factor displays an enormous sensitivity to the magnitude of the AMM [31]. By involving two vector particles, quantifiable effects would arise in the case of the two-photon TFFs too [38]. Thus, as we shall discuss in the upcoming section, this would have an impact on the low-energy domain of the $\gamma^* \pi^0 \gamma$ process, and so on the chiral anomaly.

III. $\gamma^* \pi^0 \gamma$ PROCESS AND THE CHIRAL ANOMALY

Let us now focus on the $\gamma^* \pi^0 \gamma$ transition process, which is parametrized by the matrix element (with e being the unit charge),
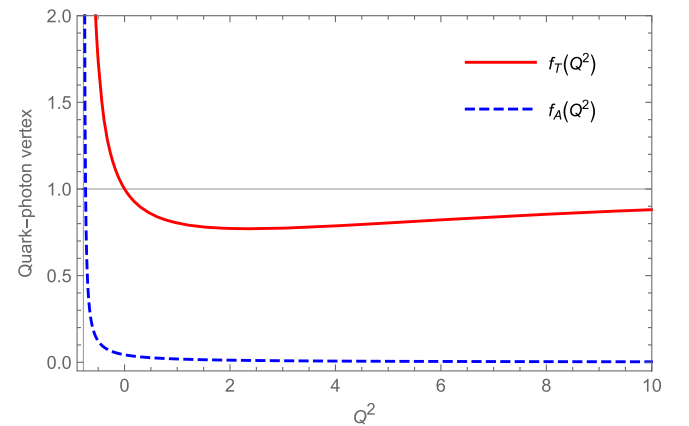
FIG. 1. Transverse QPV dressing functions defined in Eqs. (15) and (16). The function $f_A(Q^2)$ dresses the AMM contribution.

$$T_{\mu\nu}(k_1, k_2) = \frac{e^2}{4\pi^2 f_\pi} \epsilon_{\mu\nu k_1 k_2} G(k_1^2, k_1 \cdot k_2, k_2^2); \quad (19)$$

here $\epsilon_{\mu\nu k_1 k_2} = \epsilon_{\mu\nu\alpha\beta} k_{1\alpha} k_{2\beta}$ is understood. In the impulse approximation, this transition is expressed as [37–39]

$$T_{\mu\nu}(k_1, k_2) = \mathrm{tr} \int_q i\Gamma_\nu(k_2) S(q - k_2)$$
$$\times \Gamma_\pi(P) S(q + k_1) i\Gamma_\mu(k_1) S(q), \quad (20)$$

where the trace tr is taken over the Dirac indices and $P = -(k_1 + k_2)$ is the pion's total momentum, such that $P^2 = -m_\pi^2$. If k_1 denotes the momentum of the off-shell photon, then the corresponding kinematic constraints read

$$k_1^2 = Q^2, \quad k_2^2 = 0, \quad k_1 \cdot k_2 = -(Q^2 + m_\pi^2)/2. \quad (21)$$

By adopting these kinematics, the $G^{\gamma^* \pi^0 \gamma}(Q^2)$ TFF is then defined as

$$G^{\gamma^* \pi^0 \gamma}(Q^2) = 2G(Q^2, -(Q^2 + m_\pi^2)/2, 0), \quad (22)$$

where the factor 2 appears in order to account for the possible ordering of the photons.

With all the elements entering Eq. (20), namely, the quark propagator, pion BSA, and quark-photon vertex determined in Sec. II, it is, in principle, straightforward to compute this transition. However, certain ambiguities caused by the definition of the γ_5 matrix arise in treatments that require a regularization scheme. In particular, the trace involving odd numbers of γ_5 matrices leads to different results, as can be seen in Eqs. (3.11), (3.13), and (3.16) from Ref. [54]. Although it can be proved that these different results can be transformed into one another, the adopted definition of γ_5 might influence the final outcomes, and so is the case of the chiral anomaly. To overcome these issues, Ref. [54] suggests the following definition of γ_5:

$$\gamma_5 = -\frac{1}{24} \epsilon_{abcd} \gamma_a \gamma_b \gamma_c \gamma_d, \quad (23)$$

to evaluate traces that contain odd number of γ_5, so we will adopt this choice in the following.

Let us first focus on the chiral anomaly, which is associated with on-shell photon ($Q^2 = 0$) and chiral limit pion ($m_\pi = 0$), i.e., $G(0, 0, 0)$. The computed result might be represented as

$$\frac{1}{4\pi^2 f_\pi} G(0, 0, 0) = \frac{4N_c}{3M} (G_E(0, 0, 0) E_\pi + G_F(0, 0, 0) F_\pi),$$
$$(24)$$

where

$$G_E(0, 0, 0) = M^2 I_{-2}(M^2) f_T^2(0)$$
$$+ [I_0(M^2) + 4M^2 I_{-2}(M^2)] f_T(0) f_A(0)$$
$$+ [I_0(M^2) + 4M^2 I_{-2}(M^2)] f_A^2(0), \quad (25)$$

$$G_F(0, 0, 0) = 0. \quad (26)$$

The first thing to note is that the pseudovector component of the pion BSA F_π does not contribute to the anomaly. This has been shown to be the case for any symmetry-preserving treatment, based upon DSEs and BSEs, of the pion TFF [55]. By employing the regularization scheme introduced in Ref. [48], the present computation of the pion TFF falls upon this category.

Focusing on the nonvanishing contribution G_E, the last two lines in Eq. (25) reveal that the AMM term in the QPV indeed contributes to the chiral anomaly. To address this observation, let us consider the $\xi = 0$ limit, corresponding to the CI-RL result [8],

$$G^{\xi=0}(0, 0, 0) = 16\pi^2 M^2 I_{-2}(M^2), \quad (27)$$

where we have employed Eq. (13). Since $I_{-2}(M^2)$ is convergent, one can take the limits $\tau_{uv} \to 0$, $\tau_{ir} \to \infty$, and find out that

$$I_{-2}(M^2)|_{\tau_{uv} \to 0}^{\tau_{ir} \to \infty} = \frac{1}{16\pi^2} \frac{1}{2M^2}. \quad (28)$$

Thus, it turns out that the famous chiral anomaly is recovered by removing the cutoffs,

$$G^{\xi=0}(0, 0, 0)|_{\tau_{uv} \to 0}^{\tau_{ir} \to \infty} = \frac{1}{2}. \quad (29)$$

Thus, as we have seen, the chiral anomaly would only be recovered after the cutoffs are eliminated. However, in an effective theory, the ultraviolet cutoff is part of the theory itself and, in principle, must not be removed. Under such circumstances, $G^{\xi=0}(0, 0, 0) \neq \frac{1}{2}$, thus failing at meeting the value dictated by the chiral anomaly. According to Ref. [4], higher-order contributions are responsible for the missing part of the anomaly. The analysis of Ref. [9] shows how sensible terms can be added to the theory in order to mimic the complex short-distance dynamics left out by the momentum cutoff. However, for these additional terms to be given this interpretation, it is necessary for their contribution to vanish when the UV cutoff is removed. Here is where the quark AMM term in the QPV, generated automatically by the MRL truncation, becomes crucial: first, according to Eq. (25), it provides a nonvanishing contribution to $G(0, 0, 0)$; second, for arbitrary ξ its contribution vanishes when the cutoffs are removed,

$$G^{\xi\neq0}(0, 0, 0)|_{\tau_{uv} \to 0}^{\tau_{ir} \to \infty} = \frac{1}{2}, \quad (30)$$
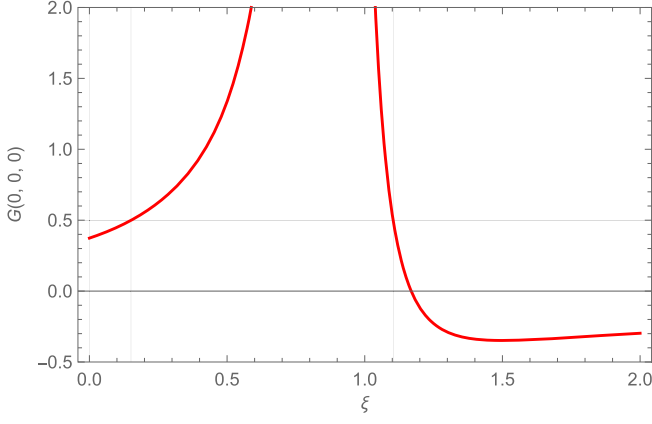
FIG. 2.   The variation of $G(0,0,0)$ as a function of the AMM strength parameter ξ.

FIG. 3. $\gamma^*\pi^0\gamma$ transition form factor. Solid curve, full computation with MRL truncation; dashed, results calculated with RL truncation; dash-dotted, results obtained with bare QPV. The dotted curve corresponds to a monopole fit to the QCD-based result in Ref. [37]. Experimental data from Refs. [56,57], brown polygons and orange disks, respectively. Mass units in GeV.

i.e., it can be duly identified as an effective term that properly encodes the short-distance dynamics beyond the cutoff. Thus, we can readily fix the strength parameter ξ by requiring $G(0,0,0) = \frac{1}{2}$ with finite cutoffs. The variation of $G(0,0,0)$ with ξ is depicted in Fig. 2. It is seen that $G(0,0,0) = \frac{1}{2}$ is, in fact, obtained from two possible values of ξ. Nonetheless, the largest one is unphysical since the ρ meson BSE yields no bound-state solutions in this case. We therefore adopt the smallest value $\xi = 0.151$ and employ it to evaluate the two-photon TFF.

To investigate the contributions of the difference pieces of the QPV on the $\gamma^*\pi^0\gamma$ TFF, the latter is computed in three different cases: by employing the *complete* QPV derived from Eq. (15) (with our preferred value $\xi = 0.151$), by taking the CI-RL truncation limit (corresponding to $\xi = 0$), thus neglecting the quark AMM contribution, and by simply plugging in the tree-level form of the QPV, thus discharging the AMM term and vector meson pole contributions. The resulting form factors are shown in Fig. 3, and the explicit mathematical expressions are presented in Appendix B. Clearly, having retained the cutoffs, the second and third cases (RL and tree-level vertices, respectively) fail to obtain the correct normalization of the form factor. This is not the case when the quark AMM is properly incorporated; not only the correct normalization is obtained (thus reproducing the chiral anomaly), but the TFF exhibits the steepest falloff among the three cases, becoming practically indistinguishable from the realistic QCD-based computations [37–39] in the small Q^2 domain. Conversely, it is conspicuously visible that the influence of the dressing functions becomes more irrelevant with increasing photon virtuality, and the hardness of the TFFs prevails in any case. This outcome is expected due to the momentum-independent nature of the CI model [8,10].

At the $Q^2 \to 0$ limit, in the MRL case, we also compute the neutral pion decay width and the corresponding

interaction radius. These are defined, respectively, as follows [37]:

$$\Gamma_{\pi^0\gamma\gamma} = \frac{g_{\pi\gamma\gamma}^2(Q^2)\alpha_{em}^2 m_\pi^3}{16\pi^3 f_\pi^2}\bigg|_{Q^2=0}, \qquad (31)$$

$$r_{\pi^0}^2 = -6\frac{d}{dQ^2}\ln g_{\pi\gamma\gamma}(Q^2)|_{Q^2=0}, \qquad (32)$$

where $g_{\pi\gamma\gamma}(Q^2) = G^{\xi=0.151}(Q^2, -(Q^2+m_\pi^2)/2, 0)$ and $\alpha_{em} = 1/137$. Equation (31) yields $\Gamma = 7.21$ eV, in agreement with the experimental determination $\Gamma = 7.82 \pm 0.14 \pm 0.17$ eV [58]. This compatibility is not surprising since, by satisfying the anomaly in the chiral limit, the prediction at the physical pion mass becomes practically independent of the model inputs. Furthermore, the interaction radius computed from Eq. (32) is $r_{\pi^0} = 0.61$ fm, which is also in fair agreement with the experimental estimate $r_{\pi^0} = 0.65 \pm 0.03$ fm [56]. The presence of the quark AMM is crucial in this case, otherwise the produced value of r_{π^0} would be practically halved [8].

IV. CONCLUSION

In this work we have computed the $\gamma^*\pi^0\gamma$ TFF, intimately connected with the so-called chiral anomaly in the Standard Model, as well as the associated decay width and interaction radius. The calculation is based upon a symmetry-preserving model of QCD, embedded within the so-called MRL truncation. In addition to the soundness of the RL approximation to address static and structural properties of pseudoscalar mesons, the MRL scheme enables the CI to produce a quark AMM term in the QPV. While RL and MRL would produce the same static properties of the pion (Table I), the presence of the quark AMM would be crucial

in the evaluation of the two-photon TFF and, in particular, in correctly reproducing the chiral anomaly.

Let us now recall that, in effective field theories, the chiral anomaly might be compromised due to the presence of finite cutoffs [4,9], whose presence could neglect complex dynamics that otherwise would have an effect on the anomaly. It is argued that such higher-order effects can be encoded in additional terms that must vanish when the cutoffs are removed [9]. This is the case of the quark AMM. To support this statement, first note that in the computation of the TFF only the leading component of the pion BSA E_π contributes to the anomaly, i.e., $G_F(0,0,0) = 0$. This is nothing but a consequence of the symmetry-preserving regularization treatment of the CI described herein. On the other hand, the quark AMM does indeed contribute to the normalization of the form factor; thereby, the strength parameter ξ can be tuned to produce, $G(0,0,0) = 1/2$, as imposed by the anomaly. Furthermore, when the cutoffs are removed, the contribution arising from the AMM vanishes regardless of the value of ξ. This is sufficient to adopt for this piece the interpretation of Ref. [9]: the AMM term could be adequately regarded as an effective term that simulates the physics discarded by the cutoffs. This interpretation becomes even more natural due to the fact that both chiral anomaly and quark AMM are strongly influenced by the effects of DCSB [51–53].

Our numerical evaluation of the $\gamma^*\pi^0\gamma$ transition included three different inputs for the QPV: the fully dressed QPV obtained in connection with the CI-MRL truncation, the one derived in the CI-RL approximation (that neglects the AMM piece), and the tree-level vertex. First, let us note that the last two cases fail to reproduce the correct normalization of the form factor; it is only possible to obtain if the cutoffs are removed [8]. The CI-MRL computation, on the other hand, satisfies the chiral anomaly, while also being practically indistinguishable from the QCD-based results [37–39] at low Q^2. In this case, the values obtained for the decay widths and interaction radius are found to be compatible with the empirical determinations as well. As the virtuality of the photon grows, the QPV dressing functions cease to be relevant and the three cases are reduced to the same; in this domain of photon momentum, the form factors become harder, as one would expect from the CI model. Finally, it is important to highlight that such encouraging results for the CI-MRL case indicate the effectiveness of the idea implemented in this work in dealing with chiral anomaly in effective theories.

This is an encouraging step toward a comprehensive study of hadrons in the CI-MRL approach, among others, because of the marked influence of the AMM on transitions concerning excited states of orbital angular momentum [31] and due to a potential connection with the anomalies in the Standard Model. The immediate next step will involve calculating $\gamma\pi^\star \to \pi\pi$ TFF and studying the chiral anomaly in this process. The work on $\gamma\pi^\star \to \pi\pi$ TFF is underway.

APPENDIX A: THE PROCESS FOR SOLVING THE PION BSE

Inserting Eq. (10) into Eq. (9), the general form of the pion BSA into the corresponding BSE, one obtains the following coupled equations for the scalar functions E_π and F_π:

$$\begin{bmatrix} E_\pi \\ F_\pi \end{bmatrix} = \frac{4}{3m_G^2} \begin{bmatrix} K_{EE} & K_{EF} \\ K_{FE} & K_{FF} \end{bmatrix} \begin{bmatrix} E_\pi \\ F_\pi \end{bmatrix}. \tag{A1}$$

By taking the Dirac trace and following the aforementioned regularization procedure, the kernels can be written as [with $\omega = M^2 + u(1-u)P^2$]

$$K_{EE} = 4\int_0^1 du I_2(\omega) - 2u(1-u)P^2 I_0(\omega),$$

$$K_{EF} = 4\int_0^1 du P^2 I_0(\omega),$$

$$K_{FE} = 2\int_0^1 du M^2 I_0(\omega),$$

$$K_{FF} = -4\int_0^1 du M^2 I_0(\omega). \tag{A2}$$

Solutions to the eigenvalue equation Eq. (A1) are only found at discrete values of momentum P_i. Thus, it is convenient to introduce the eigenvalue $\lambda(P^2)$ to deal with this equation, namely,

$$\lambda(P^2)\begin{bmatrix} E_\pi \\ F_\pi \end{bmatrix} = \frac{4}{3m_G^2} \begin{bmatrix} K_{EE} & K_{EF} \\ K_{FE} & K_{FF} \end{bmatrix} \begin{bmatrix} E_\pi \\ F_\pi \end{bmatrix}. \tag{A3}$$

The smallest value P_i^2 producing $\lambda(P_i^2) = 1$ corresponds to the ground-state pion, such that $P^2 = -m_\pi^2$.

APPENDIX B: EXPLICIT EXPRESSIONS OF THE $\gamma^*\pi^0\gamma$ TFF

With the kinematic constraints (21), the transition form factor can be written as

$$\frac{1}{4\pi^2 f_\pi}G(Q^2, -(Q^2+m_\pi^2)/2, 0)$$
$$= \frac{4N_c}{3M}\int_0^1 du_1$$
$$\times \int_0^{1-u_1} du_2(G_E(Q^2, u_1, u_2)E_\pi + G_F(Q^2, u_1, u_2)F_\pi),$$
$$\tag{B1}$$

where, with $\rho(M, u_1, u_2, Q^2) = M^2 + u_1(1 - u_1)Q^2 - u_1 u_2(Q^2 + m_\pi^2)$, one gets

$$
\begin{aligned}
G_E(Q^2, u_1, u_2) = {}& 2I_{-2}(\rho)M^2 f_T^2 + \Big(2I_{-2}(\rho)u_1 Q^2 - 6I_{-2}(\rho)u_1^2 Q^2 + 4I_{-2}(\rho)u_1^3 Q^2 + 8I_{-2}(\rho)u_1^2 u_2 Q^2 - 6I_{-2}(\rho)u_1 u_2 Q^2 \\
& + 4I_{-2}(\rho)u_1 u_2^2 Q^2 + 3I_0 u_1 + 3I_0 u_2 + 8I_{-2}(\rho)M^2 + 4I_{-2}(\rho)u_1^2 u_2 m_\pi^2 \\
& - 4I_{-2}(\rho)u_1 u_2 m_\pi^2 + 4I_{-2}(\rho)u_1 u_2^2 m_\pi^2\Big)f_A f_T + \big(2I_{-2}u_1 Q^2 - 4I_{-2}u_1^2 Q^2 - 4I_{-2}u_1 u_2 Q^2 + 2I_0 \\
& + 8I_{-2}M^2 - 4I_{-2}u_1 u_2 m_\pi^2\Big)f_A^2
\end{aligned}
$$

$$
\begin{aligned}
G_F(Q^2, u_1, u_2) = {}& (6I_{-2}(\rho)u_1 Q^2 - 10I_{-2}(\rho)u_1^2 Q^2 + 4I_{-2}(\rho)u_1^3 Q^2 + 8I_{-2}(\rho)u_1^2 u_2 Q^2 - 10I_{-2}(\rho)u_1 u_2 Q^2 + 4I_{-2}(\rho)u_1 u_2^2 Q^2 \\
& - 2I_0(\rho) + 3I_0(\rho)u_1 + 3I_0(\rho)u_2 + 4I_{-2}(\rho)u_1^2 u_2 m_\pi^2 - 8I_{-2}(\rho)u_1 u_2 m_\pi^2 + 4I_{-2}(\rho)u_1 u_2^2 m_\pi^2)f_T^2 \\
& + (2I_{-2}(\rho)Q^2 + 6I_{-2}(\rho)u_1 Q^2 - 8I_{-2}(\rho)u_1^2 Q^2 - 8I_{-2}(\rho)u_1 u_2 Q^2 - 2I_{-2}(\rho)u_2 Q^2 - 2I_{-2}(\rho)u_1 m_\pi^2 \\
& - 8I_{-2}(\rho)u_1 u_2 m_\pi^2 - 2I_{-2}(\rho)u_2 m_\pi^2)f_T f_A + \Big(-I_0(\rho)u_1 \frac{Q^2}{M^2} + 4I_{-2}(\rho)Q^2 + 2I_{-2}(\rho)u_1 \frac{Q^4}{M^2} \\
& - 4I_{-2}(\rho)u_1 Q^2 - 6I_{-2}(\rho)u_1^2 \frac{Q^4}{M^2} + 4I_{-2}(\rho)u_1^3 \frac{Q^4}{M^2} + 8I_{-2}(\rho)u_1^2 u_2 m_\pi^2 \frac{Q^2}{M^2} + 6I_{-2}(\rho)u_1^2 u_2 \frac{Q^4}{M^2} \\
& - 4I_{-2}(\rho)u_1 u_2 m_\pi^2 \frac{Q^2}{M^2} - 4I_{-2}(\rho)u_1 u_2 \frac{Q^4}{M^2} + 4I_{-2}(\rho)u_1 u_2^2 m_\pi^2 \frac{Q^2}{M^2} + 2I_{-2}(\rho)u_1 u_2^2 \frac{Q^4}{M^2} - 4I_{-2}(\rho)u_2 Q^2 \\
& - 4I_{-2}(\rho)u_1 m_\pi^2 + 2I_{-2}(\rho)u_1^2 u_2 \frac{m_\pi^4}{M^2} + 2I_{-2}(\rho)u_1 u_2^2 \frac{m_\pi^4}{M^2} - 4I_{-2}(\rho)u_2 m_\pi^2\Big)f_A^2
\end{aligned} \tag{B2}
$$

[1] J. S. Bell and R. Jackiw, A PCAC puzzle: $\pi^0 \to \gamma\gamma$ in the σ model, Nuovo Cimento A **60**, 47 (1969).

[2] S. L. Adler, Axial vector vertex in spinor electrodynamics, Phys. Rev. **177**, 2426 (1969).

[3] A. H. Blin, B. Hiller, and M. Schaden, Electromagnetic form-factors in the Nambu–Jona-Lasinio model, Z. Phys. A **331**, 75 (1988).

[4] R. Alkofer and H. Reinhardt, The chiral anomaly and electromagnetic pion decay in effective quark models, arXiv:hep-ph/9212238.

[5] V. Bernard, A. H. Blin, B. Hiller, U. G. Meissner, and M. C. Ruivo, Strong and radiative meson decays in a generalized Nambu–Jona-Lasinio model, Phys. Lett. B **305**, 163 (1993).

[6] E. Ruiz Arriola, Pion structure at high-energies and low-energies in chiral quark models, Acta Phys. Pol. B **33**, 4443 (2002).

[7] C. Schuren, F. Doring, E. Ruiz Arriola, and K. Goeke, Vector mesons in the Nambu–Jona-Lasinio model, Nucl. Phys. **A565**, 687 (1993).

[8] H. L. L. Roberts, C. D. Roberts, A. Bashir, L. X. Gutierrez-Guerrero, and P. C. Tandy, Abelian anomaly and neutral pion production, Phys. Rev. C **82**, 065202 (2010).

[9] G. P. Lepage, How to renormalize the Schrodinger equation, in *Proceedings of the 8th Jorge Andre Swieca Summer School on Nuclear Physics* (World Scientific Publishing, Singapore, 1997), pp. 135–180, arXiv:nucl-th/9706029.

[10] L. X. Gutierrez-Guerrero, A. Bashir, I. C. Cloet, and C. D. Roberts, Pion form factor from a contact interaction, Phys. Rev. C **81**, 065202 (2010).

[11] T. Frederico, Null plane model of three bosons with zero range interaction, Phys. Lett. B **282**, 409 (1992).

[12] C. D. Roberts and A. G. Williams, Dyson-Schwinger equations and their application to hadronic physics, Prog. Part. Nucl. Phys. **33**, 477 (1994).

[13] C. S. Fischer, QCD at finite temperature and chemical potential from Dyson–Schwinger equations, Prog. Part. Nucl. Phys. **105**, 1 (2019).

[14] G. Eichmann, H. Sanchis-Alepuz, R. Williams, R. Alkofer, and C. S. Fischer, Baryons as relativistic three-quark bound states, Prog. Part. Nucl. Phys. **91**, 1 (2016).

[15] S.-X. Qin, C. D. Roberts, and S. M. Schmidt, Spectrum of light-and heavy-baryons, Few-Body Syst. **60**, 1 (2019).

[16] Z.-F. Cui, M. Ding, F. Gao, K. Raya, D. Binosi, L. Chang, C. D. Roberts, J. Rodríguez-Quintero, and S. M. Schmidt, Kaon and pion parton distributions, Eur. Phys. J. C **80**, 1 (2020).

[17] J. Arrington, C. A. Gayoso, P. C. Barry, V. Berdnikov, D. Binosi, L. Chang, M. Diefenthaler, M. Ding, R. Ent, T. Frederico *et al.*, Revealing the structure of light pseudoscalar mesons at the electron–ion collider, J. Phys. G **48**, 075106 (2021).

[18] C. D. Roberts, Hadron structure using continuum Schwinger function methods, Few-Body Syst. **64**, 51 (2023).

[19] E. E. SALPETER and H. A. BETHE, A relativistic equation for bound-state problems, Phys. Rev. **84**, 1232 (1951).

[20] L. D. Faddeev, The resolvent of the schrodinger operator for a system of three particles interacting in pairs, Sov. Phys. Dokl. **6**, 384–386 (1961).

[21] L. Chang and C. D. Roberts, Sketching the Bethe-Salpeter kernel, Phys. Rev. Lett. **103**, 081601 (2009).

[22] S.-X. Qin and C. D. Roberts, Resolving the Bethe-Salpeter kernel, Chin. Phys. Lett. **38**, 071201 (2021).

[23] D. J. Wilson, I. C. Cloet, L. Chang, and C. D. Roberts, Nucleon and Roper electromagnetic elastic and transition form factors, Phys. Rev. C **85**, 025205 (2012).

[24] H. L. L. Roberts, L. Chang, I. C. Cloet, and C. D. Roberts, Masses of ground and excited-state hadrons, Few-Body Syst. **51**, 1 (2011).

[25] H. L. L. Roberts, A. Bashir, L. X. Gutierrez-Guerrero, C. D. Roberts, and D. J. Wilson, π and ρ mesons, and their diquark partners, from a contact interaction, Phys. Rev. C **83**, 065206 (2011).

[26] C. Chen, L. Chang, C. D. Roberts, S. Wan, and D. J. Wilson, Spectrum of hadrons with strangeness, Few-Body Syst. **53**, 293 (2012).

[27] J. Segovia, I. C. Cloet, C. D. Roberts, and S. M. Schmidt, Nucleon and Δ elastic and transition form factors, Few-Body Syst. **55**, 1185 (2014).

[28] F. E. Serna, B. El-Bennich, and G. a. Krein, Charmed mesons with a symmetry-preserving contact interaction, Phys. Rev. D **96**, 014013 (2017).

[29] J.-L. Zhang, Z.-F. Cui, J. Ping, and C. D. Roberts, Contact interaction analysis of pion GTMDs, Eur. Phys. J. C **81**, 6 (2021).

[30] L. X. Gutiérrez-Guerrero, G. Paredes-Torres, and A. Bashir, Mesons and baryons: Parity partners, Phys. Rev. D **104**, 094013 (2021).

[31] K. Raya, L. X. Gutiérrez-Guerrero, A. Bashir, L. Chang, Z.-F. Cui, Y. Lu, C. D. Roberts, and J. Segovia, Dynamical diquarks in the $\gamma^{(*)}p \to N(1535)\frac{1}{2}^-$ transition, Eur. Phys. J. A **57**, 266 (2021).

[32] P. Cheng, F. E. Serna, Z.-Q. Yao, C. Chen, Z.-F. Cui, and C. D. Roberts, Contact interaction analysis of octet baryon axial-vector and pseudoscalar form factors, Phys. Rev. D **106**, 054031 (2022).

[33] Z. Xing, M. Ding, and L. Chang, Glimpse into the pion gravitational form factor, Phys. Rev. D **107**, L031502 (2023).

[34] R. J. Hernández-Pinto, L. X. Gutiérrez-Guerrero, A. Bashir, M. A. Bedolla, and I. M. Higuera-Angulo, Electromagnetic form factors and charge radii of pseudoscalar and scalar mesons: A comprehensive contact interaction analysis, Phys. Rev. D **107**, 054002 (2023).

[35] Z. Xing, M. Ding, K. Raya, and L. Chang, A fresh look at the generalized parton distributions of light pseudoscalar mesons, arXiv:2301.02958.

[36] B. A. Zamora, E. C. Martínez, J. Segovia, and J. J. Cobos-Martínez, A contact interaction model for the η and η' mesons in a SDE-BSE approach to QCD: Masses, decay widths and transition form factors, Phys. Rev. D **107**, 114031 (2023).

[37] P. Maris and P. C. Tandy, Electromagnetic transition form-factors of light mesons, Phys. Rev. C **65**, 045211 (2002).

[38] K. Raya, L. Chang, A. Bashir, J. J. Cobos-Martinez, L. X. Gutiérrez-Guerrero, C. D. Roberts, and P. C. Tandy, Structure of the neutral pion and its electromagnetic transition form factor, Phys. Rev. D **93**, 074017 (2016).

[39] J. Chen, M. Ding, L. Chang, and Y.-x. Liu, Two photon transition form factor of $\bar{c}c$ quarkonia, Phys. Rev. D **95**, 016010 (2017).

[40] M. Ding, K. Raya, D. Binosi, L. Chang, C. D. Roberts, and S. M. Schmidt, Symmetry, symmetry breaking, and pion parton distributions, Phys. Rev. D **101**, 054014 (2020).

[41] H. J. Munczek, Dynamical chiral symmetry breaking, Goldstone's theorem and the consistency of the Schwinger-Dyson and Bethe-Salpeter Equations, Phys. Rev. D **52**, 4736 (1995).

[42] A. Bender, C. D. Roberts, and L. Von Smekal, Goldstone theorem and diquark confinement beyond rainbow ladder approximation, Phys. Lett. B **380**, 7 (1996).

[43] Z. Xing, K. Raya, and L. Chang, Quark anomalous magnetic moment and its effects on the ρ meson properties, Phys. Rev. D **104**, 054038 (2021).

[44] X. Wang, Z. Xing, J. Kang, K. Raya, and L. Chang, Pion scalar, vector, and tensor form factors from a contact interaction, Phys. Rev. D **106**, 054016 (2022).

[45] S.-x. Qin and C. D. Roberts, Impressions of the continuum bound state problem in QCD, Chin. Phys. Lett. **37**, 121201 (2020).

[46] M. A. Sultan, F. Akram, B. Masud, and K. Raya, Effect of the quark-gluon vertex on dynamical chiral symmetry breaking, Phys. Rev. D **103**, 054036 (2021).

[47] F. E. Serna, C. Chen, and B. El-Bennich, Interplay of dynamical and explicit chiral symmetry breaking effects on a quark, Phys. Rev. D **99**, 094027 (2019).

[48] Z. Xing and L. Chang, Symmetry preserving contact interaction treatment of the kaon, Phys. Rev. D **107**, 014019 (2023).

[49] L. Albino, A. Bashir, L. X. G. Guerrero, B. E. Bennich, and E. Rojas, Transverse Takahashi identities and their implications for gauge independent dynamical chiral symmetry breaking, Phys. Rev. D **100**, 054028 (2019).

[50] P. Maris and P. C. Tandy, The quark photon vertex and the pion charge radius, Phys. Rev. C **61**, 045202 (2000).

[51] C. D. Roberts, Electromagnetic pion form-factor and neutral pion decay width, Nucl. Phys. **A605**, 475 (1996).

[52] L. Chang, Y.-X. Liu, and C. D. Roberts, Dressed-Quark Anomalous Magnetic Moments, Phys. Rev. Lett. **106**, 072001 (2011).

[53] A. Bashir, R. Bermudez, L. Chang, and C. D. Roberts, Dynamical chiral symmetry breaking and the fermion–gauge-boson vertex, Phys. Rev. C **85**, 045205 (2012).

[54] Y.-L. Ma and Y.-L. Wu, Anomaly and anomaly-free treatment of QFTs based on symmetry-preserving loop regularization, Int. J. Mod. Phys. A **21**, 6383 (2006).

[55] P. Maris and C. D. Roberts, Pseudovector components of the pion, $\pi^0 \to \gamma\gamma$, and $F_\pi(q^2)$, Phys. Rev. C **58**, 3659 (1998).

[56] H. J. Behrend *et al.* (CELLO Collaboration), A measurement of the π^0, η, and η' electromagnetic form-factors, Z. Phys. C **49**, 401 (1991).

[57] J. Gronberg, T. Hill, R. Kutschke, D. Lange, S. Menary, R. Morrison, H. Nelson, T. Nelson, C. Qiao, J. Richman *et al.*, Measurements of the meson-photon transition form factors of light pseudoscalar mesons at large momentum transfer, Phys. Rev. D **57**, 33 (1998).

[58] R. L. Workman *et al.* (Particle Data Group), Review of particle physics, Prog. Theor. Exp. Phys. **2022**, 083C01 (2022).